

Functional expression and FRET analysis of green fluorescent proteins fused to G-protein subunits in rat sympathetic neurons

Victor Ruiz-Velasco and Stephen R. Ikeda

Laboratory of Molecular Physiology, 1 Guthrie Square, Sayre, PA 18840, USA

(Resubmitted 3 August 2001; accepted 4 September 2001)

1. cDNA constructs coding for a yellow-emitting green fluorescent protein (GFP) mutant fused to the N-terminus of the G-protein subunit $\beta 1$ (YFP- $\beta 1$) and a cyan-emitting GFP mutant fused to the N-terminus of the G-protein subunit $\gamma 2$ (CFP- $\gamma 2$) were heterologously expressed in rat superior cervical ganglion (SCG) neurons following intranuclear injection of the tagged subunits. The ability of the tagged subunits to modulate effectors, form a heterotrimer and couple to receptors was characterized using the whole-cell patch-clamp technique. Fluorescent resonance energy transfer (FRET) was also measured to determine the protein–protein interaction between the two fusion proteins.
2. Similar to co-expression of untagged $\beta 1/\gamma 2$, co-expression of YFP- $\beta 1/\gamma 2$, $\beta 1$ /CFP- $\gamma 2$, or YFP- $\beta 1$ /CFP- $\gamma 2$ resulted in a significant increase in basal N-type Ca^{2+} channel facilitation when compared to uninjected neurons. Furthermore, the noradrenaline (NA)-mediated inhibition of Ca^{2+} channels was significantly attenuated.
3. Co-expression of YFP- $\beta 1$ /CFP- $\gamma 2$ with G-protein-gated inwardly rectifying K^+ channels (GIRK1 and GIRK4) resulted in tonic GIRK currents that were blocked by Ba^{2+} .
4. The ability of the tagged subunits to form heterotrimers was tested by co-injecting either tagged or untagged $G\beta 1$ and $G\gamma 2$ with excess $G\alpha_{\text{oA}}$ cDNA. Under these conditions, the NA-mediated Ca^{2+} current inhibition was significantly decreased when compared to uninjected neurons.
5. Coupling to the $\alpha 2$ -adrenergic receptor was reconstituted in neurons expressing pertussis toxin (PTX)-insensitive $G\alpha_{\text{oA}}$ and either tagged or untagged $G\beta 1\gamma 2$ subunits. Application of NA to PTX-treated cells resulted in a voltage-dependent inhibition of N-type Ca^{2+} currents.
6. FRET measurements in the SCG revealed an *in vivo* interaction between YFP- $\beta 1$ and CFP- $\gamma 2$. Co-expression of untagged $\beta 1$ significantly decreased the interaction between the two fusion proteins.
7. In summary, the attachment of GFP mutants to the N-terminus of $G\beta 1$ or $G\gamma 2$ does not qualitatively impair their ability to form a heterotrimer, modulate effectors (N-type Ca^{2+} and GIRK channels), or couple to receptors.

The control of neuronal excitability by neurotransmitters occurs primarily through activation of G-protein-coupled receptors (GPCRs; for reviews see Hille, 1994; Ikeda & Dunlap, 1999). The most common and best-studied form of N-type Ca^{2+} channel modulation involves activation by noradrenaline (NA) of the $\alpha 2$ -adrenergic receptor ($\alpha 2$ -AR), which is coupled to pertussis toxin (PTX)-sensitive G-proteins (i.e. $G\alpha_{\text{o}}$ or $G\alpha_{\text{i}}$). Once activated, the receptor causes the dissociation of the heterotrimeric G-protein into the $G\alpha$ and $G\beta\gamma$ subunits. The result is a distinct form of N-type Ca^{2+} channel modulation that is voltage dependent and membrane delimited. This modulation is mediated by $G\beta\gamma$, as demonstrated by

Ikeda (1996) and Herlitze *et al.* (1996). It is now evident that all five known $G\beta$ subunits with various $G\gamma$ subunits are capable of producing voltage-dependent inhibition of N- and P/Q-type Ca^{2+} channels (Arnot *et al.* 2000; Ruiz-Velasco & Ikeda, 2000; Zhou *et al.* 2000). $G\beta\gamma$ also mediates the activation of G-protein-gated inwardly rectifying K^+ (GIRK) channels (Logothetis *et al.* 1987; Huang *et al.* 1995; Kofuji *et al.* 1995). Recently, it has been reported that $G\beta 1$ – $\beta 4$ and several $G\gamma$ subunits are able to tonically activate GIRK channels (Lei *et al.* 2000; Ruiz-Velasco & Ikeda, 2000).

The voltage-dependent inhibition of N-type Ca^{2+} channels appears to result from the interaction of $G\beta\gamma$ with several

sites on the Ca²⁺ channel Ca_v2.2 subunit (for reviews see Dolphin, 1998; Ikeda & Dunlap, 1999). As an initial approach towards visualizing the interaction between Gβγ and Ca²⁺ channels, the purpose of the present study was to determine the functional impact of tagging green fluorescent protein (GFP) mutants to the N-termini of Gβ1 and Gγ2. Although GFP is a valuable research tool for the study of protein localization and gene expression, its most powerful attribute comes from genetically modified mutants, which have distinct spectral properties (for review see Tsien, 1998). These properties can be exploited to monitor protein–protein interactions with the aid of fluorescence resonance energy transfer (FRET).

Yellow-emitting and cyan-emitting GFP mutants (yellow fluorescent protein, YFP and cyan fluorescent protein, CFP, respectively) were fused in-frame to the N-terminus of Gβ1 (YFP-β1) and Gγ2 (CFP-γ2), respectively. Rat superior cervical ganglion (SCG) neurons were microinjected with both cDNA constructs, and the properties of the expressed G-protein subunits were examined. The ability of the two tagged subunits to form a functional dimer and modulate effectors (i.e. N-type Ca²⁺ and GIRK channels) was tested by using the patch-clamp technique. Whether YFP-β1 and CFP-γ2 were capable of forming a heterotrimer with GDP-bound Gα_{oA} was also studied. Coupling of the tagged subunits and PTX-insensitive Gα subunits to α2-ARs was determined by measuring receptor-mediated voltage-dependent Ca²⁺ channel inhibition. Finally, FRET measurements between the two tagged G-protein subunits was employed. The electrophysiological and FRET results presented show that attachment of the mutant GFP to the N-terminus of either Gβ1 or Gγ2 does not interfere with their ability to form functional dimers or interact with effectors or receptors. Thus, GFP-labelled β1γ2 may prove useful for quantifying expression levels, monitoring localization and measuring the dynamic interaction between Gβγ and effector and/or receptor proteins.

METHODS

Neuron isolation

Single neurons from the adult rat SCG were prepared using a method that has been described previously (Ruiz-Velasco & Ikeda, 2000). The experiments carried out were approved by the Institutional Animal Care and Use Committee (IACUC). Male Wistar rats (175–225 g) were anaesthetized with CO₂ and then decapitated using a laboratory guillotine. Cell isolation was then carried out (see Ruiz-Velasco & Ikeda, 2000). The dispersed neurons were resuspended in minimal essential medium (MEM; Mediatech, Herndon, VA, USA), supplemented with 10% fetal calf serum (Atlanta Biologicals, Atlanta, GA, USA), 1% glutamine and a 1% penicillin–streptomycin solution (both from Mediatech). The neurons were then plated onto 35 mm tissue culture plates coated with poly-L-lysine and stored in a humidified incubator containing 5% CO₂ in air at 37 °C.

cDNA microinjection

Microinjection of cDNA plasmids was performed with an Eppendorf 5246 microinjector and a 5171 micromanipulator (Madison, WI, USA) 3–5 h after plating, as described previously (Ikeda, 1997). Plasmids

coding for bovine Gβ1 and Gγ2 (both subcloned into the mammalian expression vector pCI; Promega, Madison, WI, USA) were prepared using anion-exchange columns (Qiagen, Chatsworth, CA, USA) and stored in TE buffer (10 mM Tris, 1 mM EDTA, pH 8.0). Human GIRK1 and GIRK4 (Kir 3.1 and 3.4) cDNA were supplied in pcDNA3.1 (Invitrogen, Carlsbad, CA, USA) and prepared as above. The YFP-Gβ1 cDNA (kind gift from Dr Richard J. Miller) was supplied in the ‘enhanced’ jellyfish yellow fluorescent protein vector pEYFP-C1 with an 18 amino acid linker (derived from the vector multiple cloning site). The ECFP-Gγ2 clone was constructed by linking the pECFP-CI vector to the N-terminus of the Gγ2 cDNA with a two amino acid linker. The linker sequence was TCC GGA, encoding serine (S) and glycine (G), respectively. Site-directed mutagenesis of the mouse Gα_{oA} subunit was performed using the GeneEditor *in vitro* site-directed mutagenesis kit (Promega), as described previously (Jeong & Ikeda, 2000). The codon specifying the fourth amino acid from the C-terminus, cysteine, was mutated to code for glycine (C351G). The mutation was confirmed by automated DNA sequencing (ABI 310; Perkin Elmer, Foster City, CA, USA), and the PCR product (Gα_{oA} (C351G)) was subcloned into pCI.

Electrophysiology and data analysis

Neurons receiving a successful nuclear injection of untagged Gβ1 and Gγ2 were identified by fluorescence from co-expressed GFP (pEGFP-N1, 5 ng μl⁻¹; Clontech Laboratories, Palo Alto, CA, USA). In FRET experiments, pECFP-N1 and pEYFP-N1 cDNA plasmids (both from Clontech) were microinjected at a final concentration of 5 ng μl⁻¹. Neurons expressing EGFP, ECFP, EYFP, YFP-Gβ1 and CFP-Gγ2 were identified 12–20 h later using an inverted microscope (Diaphot 300; Nikon, Tokyo, Japan) equipped with a ×40 objective (0.6 NA) and an epifluorescence unit (CFPv2 filter set; Chroma Technologies, Brattleboro, VT, USA; XF88 filter Omega Optical, Brattleboro, VT, USA). Prior to imaging or FRET detection, the MEM was replaced with external GIRK recording solution (see below). Fluorescence images were captured with a SPOT RT cooled CCD camera and software (Diagnostic Instruments, Sterling Heights, MI, USA) and processed with Adobe Photoshop software package (Adobe Systems, San Jose, CA, USA).

Ca²⁺ and GIRK currents were recorded using the whole-cell variant of the patch-clamp technique (Hamill *et al.* 1981). Patch pipettes were pulled from borosilicate glass capillaries (Corning 7052; Garner Glass, Claremont, CA, USA) on a P-97 Flaming–Brown micropipette puller (Sutter Instruments, San Rafael, CA, USA), coated with Sylgard (Dow Corning, Midland, MI, USA) and fire polished on a microforge. Whole-cell currents were acquired with a patch-clamp amplifier (Axopatch-1C, Axon Instruments, Foster City, CA, USA), analog filtered at 1–2 kHz (–3 dB; four-pole Bessel) and digitized using custom-designed software (S4) on a Power PC computer (Power Computing, Austin, TX, USA) equipped with a 16-bit A/D converter board (ITC16, Instrutech, Elmont, NY, USA). Cell membrane capacitance and series resistance (80–85%) were compensated electronically. All experiments were performed at room temperature (21–24 °C). Data and statistical analysis were performed with Igor (Lake Oswego, OR, USA) and GB-Stat PPC (Silver Spring, MD, USA) software packages, respectively, using ANOVA followed by the Newman–Keuls test or the standard *t* test. *P* < 0.05 was considered statistically significant. Graphs and current traces were produced with Igor and Canvas software packages (Deneba Software, Miami, FL, USA).

Basal facilitation (i.e. prior to NA application) was calculated as the ratio of the amplitude of the Ca²⁺ current (*I*_{Ca}), determined from the test pulse (+10 mV) occurring after (postpulse), to that of the *I*_{Ca} obtained before (prepulse) the +80 mV conditioning pulse (see Fig. 2*D*). *I*_{Ca} amplitude was measured isochronally 10 ms after the initiation of each test pulse. The NA-mediated inhibition was

calculated as follows: $(I_{Ca}(\text{prepulse before NA}) - I_{Ca}(\text{prepulse after NA})) / (I_{Ca}(\text{prepulse before NA})) \times 100$. Basal and agonist-stimulated peak GIRK currents were calculated by digitally subtracting current traces obtained before NA exposure from those obtained after application of 1 mM Ba²⁺ + 10 μM NA. Maximal inward currents normally occurred between -135 and -125 mV.

FRET analysis

Neurons expressing labelled G-protein subunits were excited with light from a mercury short arc lamp. The cells were viewed with an inverted microscope (Diaphot 300; Nikon) equipped with a ×40 objective (0.55 NA). CFP-γ2 and ECFP were observed with the following filter set: excitation filter at 436 ± 10 nm, a dichroic beam splitter of 455 nm (long pass), and an emission filter at 480 ± 10 nm (Chroma). YFP-β1 and EYFP were observed with the following filter set: excitation filter at 500 ± 12 nm, a dichroic beam splitter of 525 nm (long pass), and an emission filter at 545 ± 17 nm (Omega). The FRET filter set contained an excitation filter at 440 ± 10.5 nm, a dichroic beam splitter of 505 nm (long pass), an emission filter (for donor) at 480 ± 15 nm and a second emission filter (for acceptor) at 535 ± 13 nm (Omega). The cells were excited at 440 nm for 70 ms and the emission was acquired at 480 nm and 535 nm, with the aid of photomultipliers (Photon Technology International, Lawrenceville, NJ, USA). All emission values are expressed in volts (V). Background values employed were regions containing no cells in the viewing field.

FRET between the two fluorophores was determined as described previously by Gordon *et al.* (1998). Briefly, excitation of the donor (CFP) and acceptor (YFP) was performed with the FRET filter set and the YFP filter set, respectively. The FRET filter set was also used to obtain both the donor and acceptor fluorescence. The nomenclature (adapted from Gordon *et al.* 1998) of the fluorescence signals included the following: Dd (signal at 480 nm from cells expressing CFP using the FRET filter set), Fd (signal at 535 nm from cells expressing CFP using the FRET filter set), Ad (signal at 535 nm from cells expressing CFP using the YFP filter set), Da (signal at 480 nm from cells expressing YFP using the FRET filter set), Fa (signal at 535 nm from cells expressing YFP using the FRET filter set), Aa (signal at 535 nm from cells expressing YFP using the YFP filter set), Df (signal at 480 nm from cells expressing CFP and YFP using the FRET filter set), Ff (signal at 535 nm from cells expressing CFP and YFP using the FRET filter set) and Af (signal at 535 nm from cells expressing CFP and YFP using the YFP filter set). Fd and Ad represent cross-talk of the CFP (donor) signal, while the Fa and Da signals represent cross-talk of the YFP (acceptor) signal. However, with the filter sets employed in this study, Da and Ad were effectively zero. The Fd/Dd and Fa/Aa ratios represent the cross-talk of both the CFP emission that leaked through the FRET filter and the YFP emission due to direct excitation by the FRET filter, respectively. The Ff/Df ratio, when corrected for cross-talk from both fluorophores, is the measure of FRET between the two fluorophores. It was obtained from the emission of CFP with the FRET filter in cells expressing both CFP and YFP. In a separate group of cells (negative controls), cDNA of the non-interacting fluorophores ECFP and EYFP was co-injected at a concentration of 5 ng μl⁻¹ per fluorophore.

Solutions and drugs

For recording I_{Ca} , the pipette solution contained (mM): 120 N-methyl-D-glucamine, 20 tetraethylammonium hydroxide (TEA-OH), 11 EGTA, 10 Hepes, 10 sucrose, 1 CaCl₂, 4 MgATP, 0.3 Na₂ATP and 14 Tris creatine phosphate; pH 7.2 with methanesulphonic acid and HCl (20 mM), and 299–302 mosmol kg⁻¹. The external solution consisted of (mM): 140 methanesulphonic acid, 145 TEA-OH, 10 Hepes, 15 glucose, 10 CaCl₂ and 0.0003 TTX; pH 7.4 and 312–326 mosmol kg⁻¹. For recording GIRK currents, the pipette solution contained (mM): 135 KCl, 11 EGTA, 1 CaCl₂, 2 MgCl₂, 10 Hepes, 4 MgATP and 0.3

Na₂ATP; pH 7.2 and 299–302 mosmol kg⁻¹. The external solution consisted of (mM): 130 NaCl, 5.4 KCl, 10 Hepes, 10 CaCl₂, 0.8 MgCl₂, 15 glucose, 15 sucrose and 0.0003 TTX; pH 7.4 and 317–319 mosmol kg⁻¹.

Stock solutions of NA (bitartrate salt; Sigma Chemical) and PTX (List Biological Laboratories, Campbell, CA, USA) were prepared in H₂O. All drugs were diluted in the external solution from stock solutions to their final concentrations just prior to use. Neurons pretreated with PTX were incubated overnight (12–20 h) in tissue culture medium containing 500 ng ml⁻¹ of the toxin.

Drug application to the neuron under study was performed by positioning a custom-designed gravity-fed perfusion system ~100 μm from the cell, as described previously (Ruiz-Velasco & Ikeda, 1998). To wash off drugs and avoid flow-induced artifacts, the capillary column containing normal external solution was kept open continuously until the time when the desired solution was employed.

The results are presented as means ± S.E.M.

RESULTS

Heterologous expression of G-protein subunits YFP-β1 and CFP-γ2 results in basal inhibition of N-type I_{Ca} in rat SCG neurons

In the present study, cDNA constructs coding for G-protein β1 and γ2 subunits fused in-frame with yellow- and cyan-emitting GFP mutants, respectively, were microinjected into rat SCG neurons. Figure 1 shows phase contrast and fluorescence images of three neurons that were microinjected with YFP-β1/γ2 (*A*), β1/CFP-γ2 (*B*) and YFP-β1/CFP-γ2 cDNA (*C*; 10 ng μl⁻¹ per subunit). Fluorescence images, acquired 12–16 h following microinjection, show the successful expression of the fusion proteins. The localization pattern of the tagged subunits appeared to be membrane bound. However, the presence of cytosolic tagged subunits cannot be ruled out. Furthermore, heterologous overexpression of either fusion protein alone (Fig. 1*A* and *B*) or combined (Fig. 1*C*) did not result in any morphological alteration.

To determine whether both subunits displayed modulatory effects similar to untagged β1γ2, electrophysiological studies were performed to evaluate their ability to produce voltage-dependent inhibition of Ca²⁺ channels. Voltage-dependent modulation of N-type Ca²⁺ channels results in kinetic slowing of activation and prepulse facilitation. Figure 2*A* illustrates superimposed I_{Ca} traces from an uninjected cell before (lower trace) and after (upper trace) exposure to 10 μM NA. I_{Ca} were evoked with a double-pulse voltage protocol from a holding potential of -80 mV (shown at the bottom of Fig. 2*D*). The voltage protocol consisted of two identical test pulses (to +10 mV) separated by a large, depolarizing (to +80 mV) conditioning pulse (Ikeda, 1991). Before NA application, the current evoked during the prepulse rose rapidly and reached a plateau within 5–10 ms after the onset of the test pulse (lower trace, Fig. 2*A*). Following NA exposure, the I_{Ca} rising phase was slower and biphasic (upper trace, Fig. 2*A*). Figure 2*A* also shows that prior to the addition of NA, the postpulse current amplitude was only slightly affected by the conditioning pulse (to +80 mV). Upon NA application,

however, the postpulse current was much larger than the prepulse current, presumably as a result of voltage-dependent relief of the block during the test pulse. Basal facilitation (i.e. in the absence of NA) for uninjected neurons was 1.37 ± 0.03 ($n = 18$), and the mean NA-mediated inhibition was $59.0 \pm 2.9\%$ (Fig. 2E). Figure 2B shows I_{Ca} traces of a neuron co-injected with $\beta 1$ and $\gamma 2$ cDNA ($10 \text{ ng } \mu\text{l}^{-1}$ per subunit). As expected from previous studies (Herlitze *et al.* 1996, Ikeda, 1996; Ruiz-Velasco & Ikeda, 2000), the currents show an enhanced kinetic slowing and prepulse facilitation. Following NA application, little voltage-dependent inhibition was observed due to the near-maximal modulation caused by $\beta 1\gamma 2$ overexpression. Thus, in $\beta 1\gamma 2$ -expressing neurons (filled bars), basal facilitation significantly increased to 3.30 ± 0.10 ($n = 4$, $P < 0.01$), while the NA-mediated inhibition was significantly decreased ($6.2 \pm 2.9\%$, $P < 0.01$, Fig. 2E).

The effects of co-expressing YFP- $\beta 1$ and $\gamma 2$ (YFP- $\beta 1/\gamma 2$) and YFP- $\beta 1$ and CFP- $\gamma 2$ (YFP- $\beta 1$ /CFP- $\gamma 2$) are shown in Fig. 2C and D. As for co-expressed, untagged $\beta 1$ and $\gamma 2$, there was a significant increase in basal facilitation and an attenuation of the NA-mediated I_{Ca} inhibition in both

neurons. Figure 2E is a summary of the mean basal facilitation and NA-mediated inhibition of cells expressing either tagged or untagged $\beta 1$ and $\gamma 2$. As reported previously, the expression of $\beta 1$ and $\gamma 2$ together resulted in a significantly greater modulation of I_{Ca} than when either subunit was expressed alone (Ikeda, 1996; Ruiz-Velasco & Ikeda, 2000). Microinjection of either $\gamma 2$ or CFP- $\gamma 2$ cDNA did not produce significant differences in basal facilitation or NA-mediated inhibition when compared to uninjected neurons (Fig. 2E). On the other hand, $\beta 1$ and YFP- $\beta 1$ microinjection resulted in significant increases in basal facilitation ($P < 0.05$ and $P < 0.01$, respectively). However, the NA-mediated inhibition of I_{Ca} was not different when compared with uninjected neurons. Therefore, neither of the mutant GFP tags appears to interfere with the ability of $\beta 1\gamma 2$ to modulate Ca^{2+} channels.

Heterologously expressed YFP- $\beta 1$ and CFP- $\gamma 2$ basally activate GIRK channels

GIRK channels are also $\text{G}\beta\gamma$ -modulated effectors. However, rather than inhibiting N-type Ca^{2+} channels, $\text{G}\beta\gamma$ activates GIRK channels (Logothetis *et al.* 1987; but

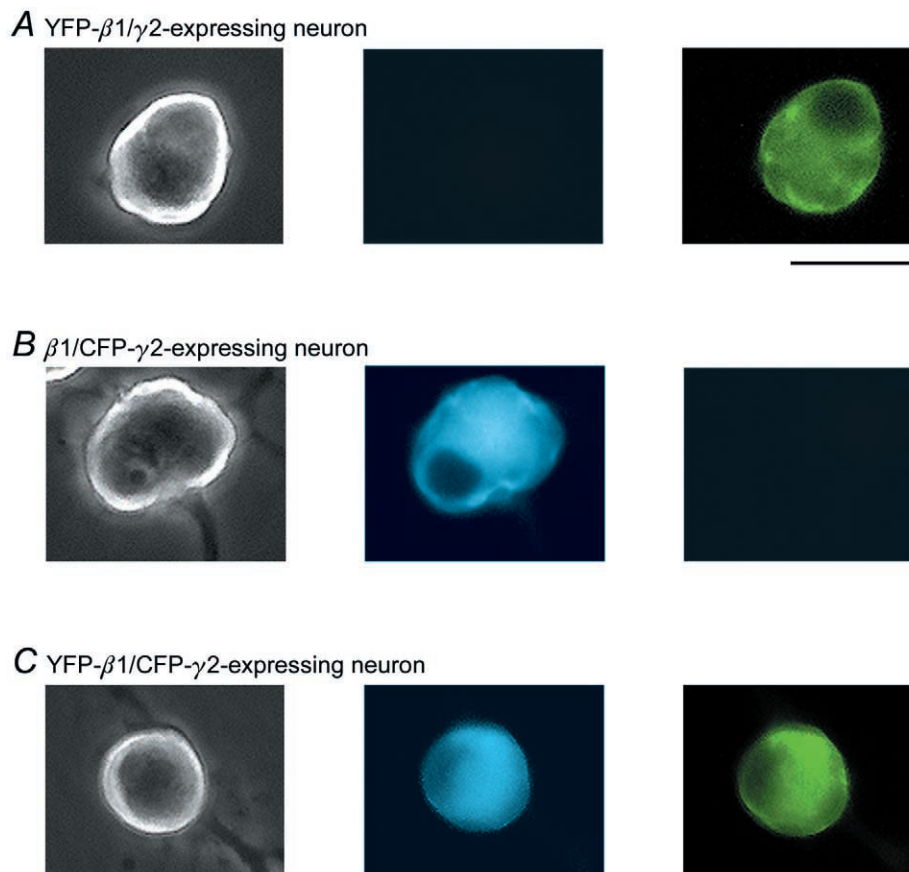


Figure 1. Heterologous expression of YFP- $\beta 1$ and CFP- $\gamma 2$ alone or in combination in adult rat SCG neurons

Phase contrast and fluorescence images of neurons expressing YFP- $\beta 1/\gamma 2$ (A), $\beta 1$ /CFP- $\gamma 2$ (B) and YFP- $\beta 1$ /CFP- $\gamma 2$ (C). Fluorescence images were taken with a filter set specific for CFP (centre panels) and YFP (right panels; 440 nm excitation, and 480 nm emission and 535 nm emission for CFP and YFP, respectively). Fluorescence images shown are pseudocoloured. Scale bar, $55 \mu\text{m}$.

see Lei *et al.* 2000). Although SCG neurons do not express native GIRK channels, robust GIRK currents can be recorded in SCG neurons heterologously expressing GIRK1, 2 and 4 channels (Kir 3.1, 3.2 and 3.4, respectively; Ruiz-Velasco & Ikeda, 1998, 2000; Fernandez-Fernandez *et al.* 1999). In this study, GIRK1 and GIRK4 channels were expressed heterologously in SCG neurons to determine whether GFP-tagged G-protein subunits activate these channels. GIRK currents were recorded every 10 s by applying 200 ms voltage ramps from -140 to -40 mV from a holding potential of -60 mV. Figure 3A shows peak GIRK current amplitude as a function of time in a neuron previously co-injected with GIRK1 and GIRK4 cDNA. Before exposure to $10 \mu\text{M}$ NA, little GIRK current was observed (a in Fig. 3A and inset). Application of NA (filled bar), however, resulted in GIRK

channel activation (b in Fig. 3A and inset). When the cell was exposed to 1 mM Ba^{2+} in the presence of NA (filled bar), the GIRK current was blocked (c in Fig. 3A and inset). Upon removal of NA and Ba^{2+} , there was a slight increase in GIRK current amplitude, which was followed by a return to control levels. This transient increase is presumably the result of a faster washout of Ba^{2+} than NA. Figure 3B and C shows peak GIRK amplitude as a function of time for two neurons expressing GIRK1 and GIRK4, with YFP- $\beta 1/\gamma 2$ and YFP- $\beta 1/\text{CFP-}\gamma 2$, respectively. Prior to NA application, both cells showed a tonic GIRK current of approximately 2 nA (Fig. 3B and C, insets). Exposure to $10 \mu\text{M}$ NA (filled bar) resulted in additional GIRK currents that were also sensitive to Ba^{2+} (see Fig. 3B and C insets). Figure 3D is a summary of basal peak GIRK currents in cells expressing GIRK1 and

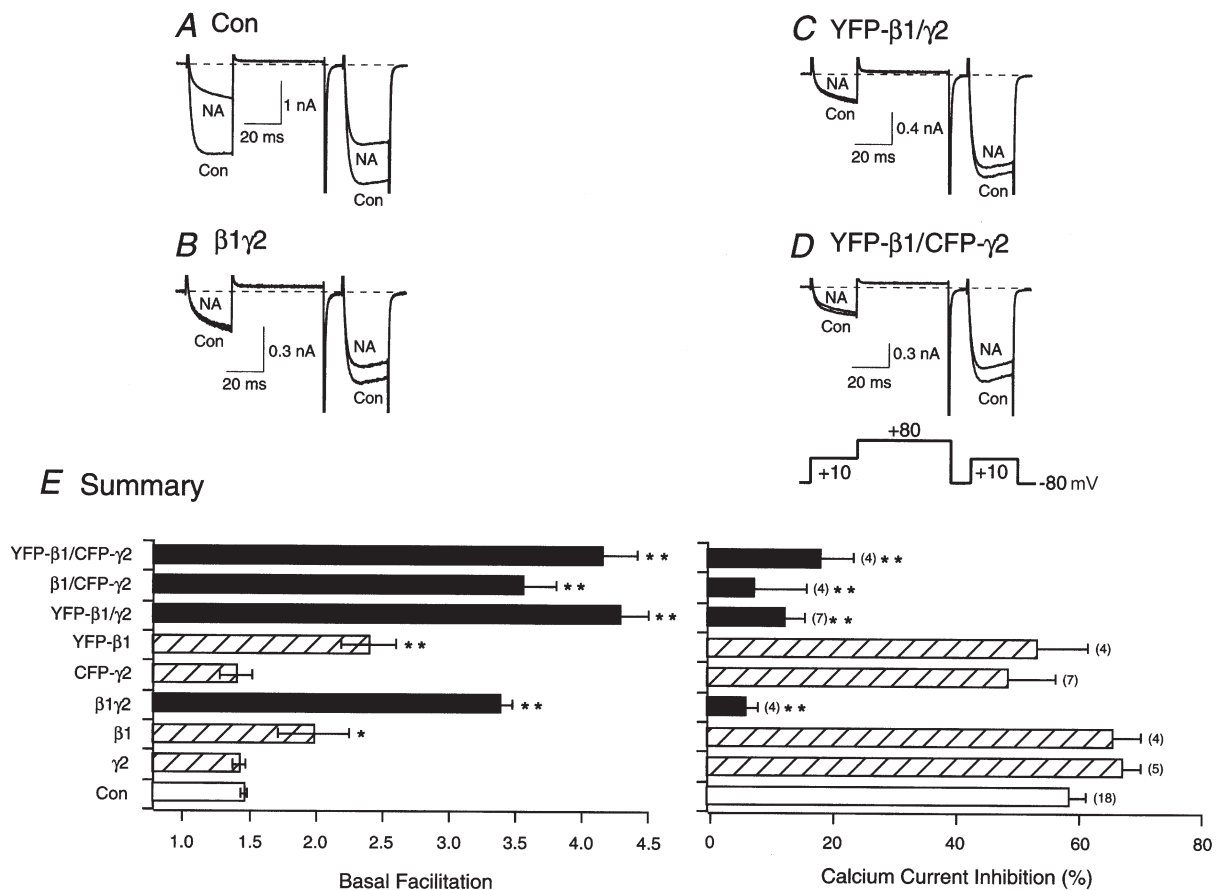


Figure 2. Effect of heterologous expression of $\beta 1$, YFP- $\beta 1$, $\gamma 2$ or CFP- $\gamma 2$ alone or in combination on facilitation and noradrenaline (NA)-mediated inhibition of I_{Ca} in SCG neurons

Superimposed I_{Ca} traces evoked with the double-pulse voltage protocol (shown at the bottom of D) in the absence (lower traces) and presence (upper traces) of $10 \mu\text{M}$ NA for control (A), $\beta 1\gamma 2$ -expressing neurons (B), YFP- $\beta 1/\gamma 2$ -expressing neurons (C) and YFP- $\beta 1/\text{CFP-}\gamma 2$ -expressing neurons (D). Currents were evoked every 10 s. Dashed lines indicate the zero current level. E, summary graphs of mean (\pm S.E.M.) basal facilitation and I_{Ca} inhibition for neurons expressing $\beta 1$, YFP- $\beta 1$, $\gamma 2$ or CFP- $\gamma 2$ alone or in combination. The final concentration of cDNA injected was 10 ng ml^{-1} per subunit. Facilitation was calculated as the ratio of I_{Ca} amplitude determined from the test pulse ($+10$ mV) occurring after (postpulse) and before (prepulse) a $+80$ mV conditioning pulse. * $P < 0.05$ and ** $P < 0.01$ vs. control (uninjected neurons, Con). Numbers in parentheses indicate the number of experiments.

GIRK4 alone and with tagged $\beta 1\gamma 2$ constructs. The results show that GIRK1 and GIRK4 expressed alone in neurons did not lead to significant basal activation of GIRK currents (0.05 ± 0.01 nA, range 0.01–0.09 nA, $n = 5$) as observed with cells expressing YFP- $\beta 1/\gamma 2$ (3.2 ± 0.9 nA, range 1.81–4.77 nA, $n = 3$), $\beta 1$ /CFP- $\gamma 2$ (6.4 ± 2.3 nA, range 1.92–12.95 nA, $n = 4$) and YFP- $\beta 1$ /CFP- $\gamma 2$ (5.8 ± 2.7 nA, range 0.42–16.11 nA, $n = 6$). Similar tonic activation of GIRK1 and GIRK4 channels has been reported previously in SCG neurons expressing untagged $\beta 1\gamma 2$ (Ruiz-Velasco & Ikeda, 2000). The data indicate that in SCG neurons the expressed GIRK channels couple to native $\alpha 2$ -ARs and utilize native and co-expressed tagged G-proteins. These results provide additional evidence that YFP- $\beta 1$ and CFP- $\gamma 2$ are capable of modulating another G $\beta\gamma$ effector (i.e. GIRK channels).

Overexpression of $G\alpha_{oA}$, YFP- $\beta 1$ and CFP- $\gamma 2$ subunits results in heterotrimer formation

Experiments were designed to determine whether both tagged $\beta 1$ and $\gamma 2$ would interact with $G\alpha$ subunits and form a heterotrimer. In rat SCG neurons, natively expressed $G\alpha_{oA}$ couples to $\alpha 2$ -ARs (Caulfield *et al.* 1994). $G\alpha_{oA}$, YFP- $\beta 1$ and CFP- $\gamma 2$ cDNA were co-injected at a ratio (weight) of approximately 10:1:1, respectively. Under these conditions, the excess GDP-bound $G\alpha_{oA}$ that is expressed should act as a G $\beta\gamma$ 'sink' due to the high affinity for the dimer, leading to the loss of effector interaction (Slepak *et al.* 1995; Ikeda, 1996; Jeong & Ikeda, 1999). Figure 4A illustrates the whole-cell I_{Ca} of an uninjected cell before and after application of 10 μ M NA. As shown previously, NA produced the typical voltage-

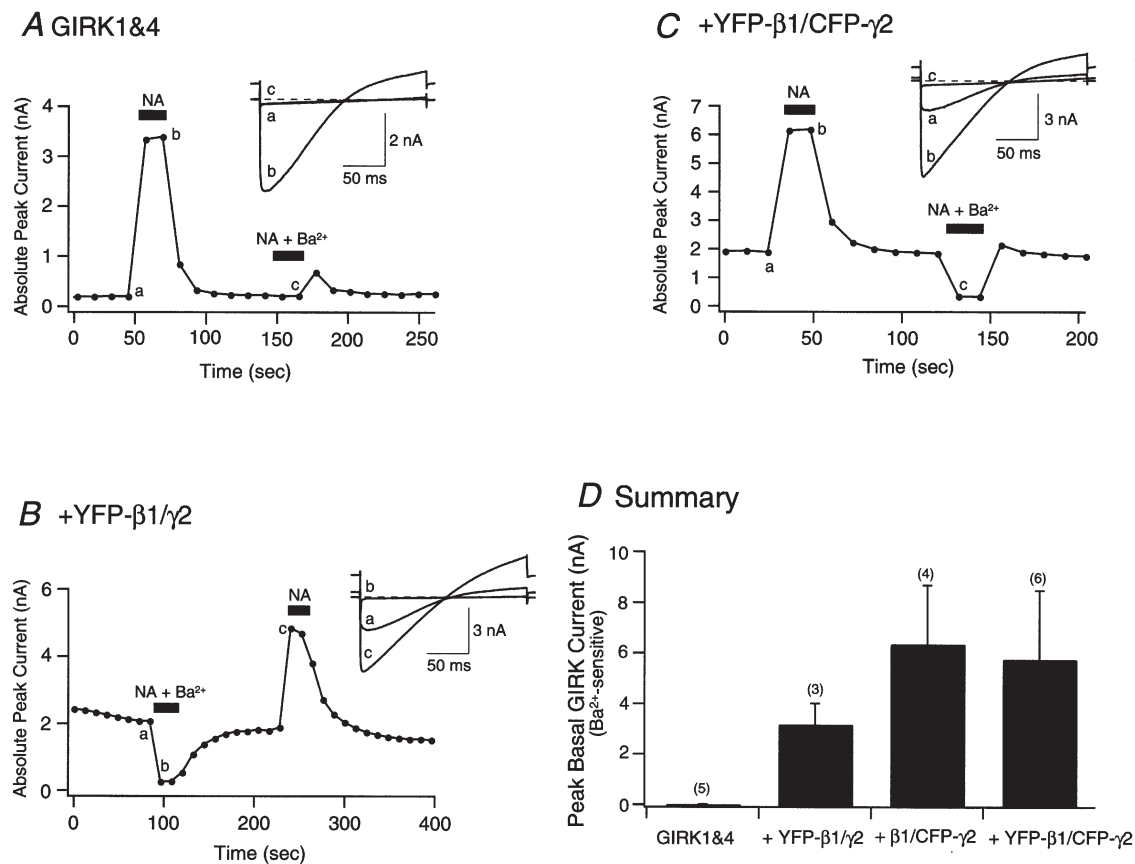


Figure 3. Effect of heterologous expression of YFP- $\beta 1/\gamma 2$, $\beta 1$ /CFP- $\gamma 2$ and YFP- $\beta 1$ /CFP- $\gamma 2$ on GIRK channel activation

Time course of basal and NA-activated GIRK channel currents in control (neurons expressing GIRK1 and GIRK4 only; *A*), GIRK1 and GIRK4 + YFP- $\beta 1/\gamma 2$ -expressing neurons (*B*) and GIRK1 and GIRK4 + YFP- $\beta 1$ /CFP- $\gamma 2$ -expressing neurons (*C*). Currents were evoked by 200 ms voltage ramps from -140 mV to -40 mV from a holding potential of -60 mV, applied every 10 s. Filled bars indicate the application of 10 μ M NA, or 1 mM Ba^{2+} + 10 μ M NA. Insets for *A* and *C* show current traces obtained before (a) and after the application of NA (b) or NA + Ba^{2+} (c). Inset for *B* shows current traces obtained before (a) and after the application of NA (c) or NA + Ba^{2+} (b). Dashed lines indicate the zero current level. *D*, summary graph showing the mean (\pm S.E.M.) basal peak GIRK currents recorded prior to NA application. Basal peak GIRK current values were obtained by subtracting the currents recorded before NA exposure from those obtained after the application of 1 mM Ba^{2+} + 10 μ M NA. Numbers in parentheses indicate the number of experiments.

dependent inhibition and kinetic slowing of the currents. The mean NA-mediated inhibition was $61.2 \pm 2.0\%$ ($n = 27$). When compared to uninjected cells, overexpression of $G\alpha_{oA}$ alone caused a decrease in basal facilitation (Fig. 4B and E). In addition, the postpulse current showed some inactivation. This is consistent with the ability of $G\alpha$ to bind free $\beta\gamma$ (Ikeda, 1996). Figure 4B and E also shows that $G\alpha_{oA}$ overexpression significantly abolished the NA-mediated I_{Ca} inhibition, presumably as a result of sequestering the $G\beta\gamma$ released following receptor activation ($4.1 \pm 1.3\%$, $n = 5$). Traces of I_{Ca} for a neuron overexpressing $\beta1/CFP-\gamma2$ before and after exposure to $10 \mu\text{M}$ NA are shown in Fig. 4C. As demonstrated before, the two subunits produced a tonic inhibition of the I_{Ca} in the absence of NA (Figs 2E and 4E). Exposure of the neuron to NA failed to produce an additional significant

decrease in I_{Ca} (Fig. 4C and E). However, when all three subunits were co-expressed (Fig. 4D), the enhanced basal facilitation produced by $\beta1/CFP-\gamma2$ was attenuated from 3.5 ± 0.3 ($n = 4$) to 1.1 ± 0.04 ($n = 4$). In addition, the NA-mediated I_{Ca} inhibition was significantly decreased ($P < 0.01$; Fig. 4E), presumably as a result of excess GDP-bound $G\alpha_{oA}$ binding the native and heterologously expressed $G\beta\gamma$ subunits. Similarly, neurons co-injected with $\beta1/\gamma2$, YFP- $\beta1/\gamma2$ and YFP- $\beta1/CFP-\gamma2$ cDNA with a 10-fold higher amount of $G\alpha_{oA}$ cDNA showed a significant ($P < 0.01$) reduction of NA-mediated I_{Ca} inhibition when compared to cells expressing tagged or untagged $G\beta1\gamma2$. Figure 4E summarizes the basal facilitation ratio and NA-mediated I_{Ca} inhibition in neurons expressing tagged and untagged $\beta1\gamma2$ constructs with (filled bars) and without (open bars) $G\alpha_{oA}$ over-

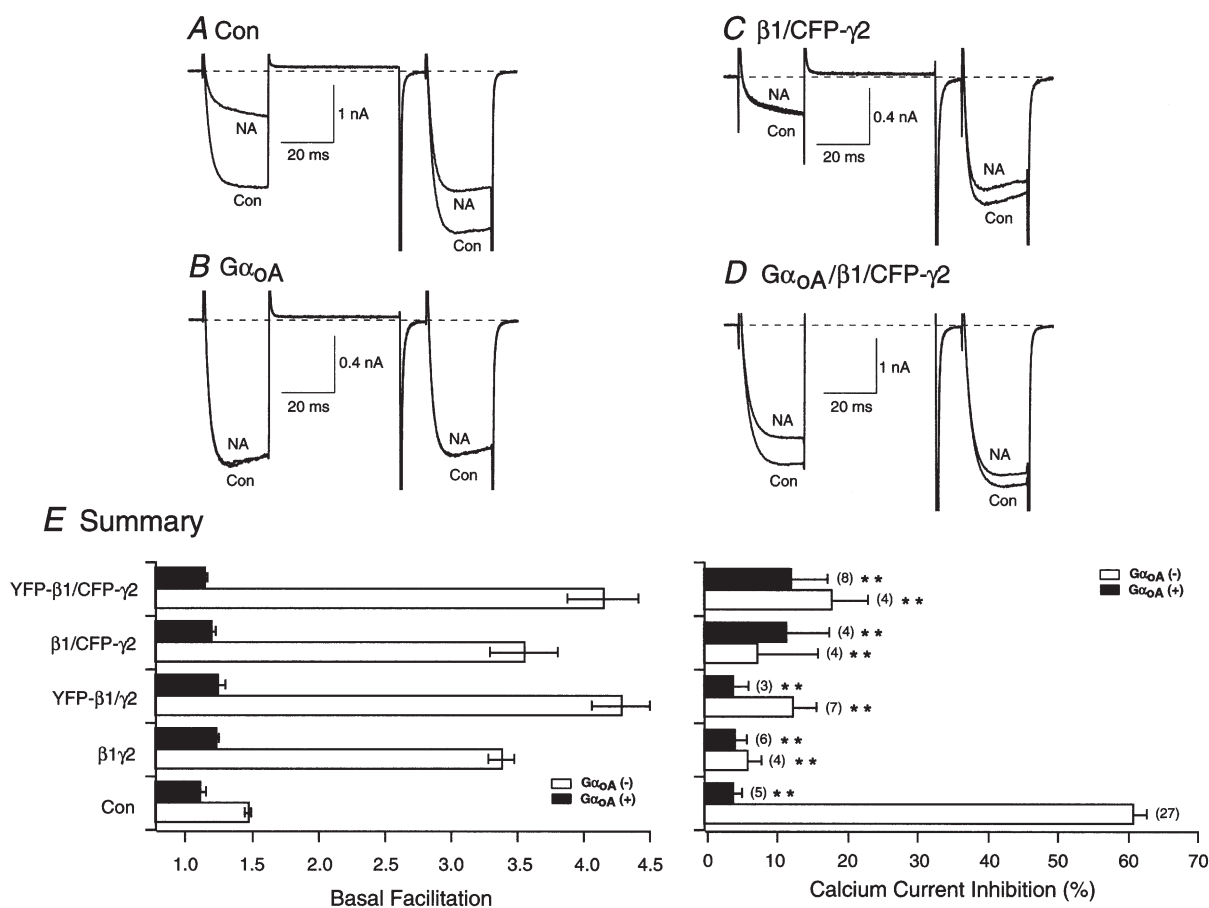


Figure 4. Heterologous overexpression of $G\alpha_{oA}$ abolishes the enhanced basal facilitation mediated by $\beta\gamma$ subunits, and blocks the NA-mediated I_{Ca} inhibition

Superimposed I_{Ca} traces evoked with the double-pulse voltage protocol (shown at the bottom of Fig. 2D) in the absence (lower traces) and presence (upper traces) of $10 \mu\text{M}$ NA for control (A), $G\alpha_{oA}$ -expressing neurons (B), $\beta1/CFP-\gamma2$ -expressing neurons (C) and $G\alpha_{oA}/\beta1/CFP-\gamma2$ -expressing neurons (D). Currents were evoked every 10 s. Dashed lines indicate the zero current level. E, summary graphs of mean (\pm S.E.M.) basal facilitation and I_{Ca} inhibition for neurons expressing $\beta1\gamma2$, YFP- $\beta1/\gamma2$, $\beta1/CFP-\gamma2$ and YFP- $\beta1/CFP-\gamma2$ with (filled bars) and without (open bars) $G\alpha_{oA}$ overexpression. Facilitation and NA-mediated inhibition were determined as described in the legend of Fig. 2. The final concentration of cDNA injected was 10 ng ml^{-1} per β and γ subunit, and 100 ng ml^{-1} for the α subunit. ** $P < 0.01$ vs. non- $G\alpha_{oA}$ -expressing control neurons (Con). Numbers in parentheses indicate the number of experiments.

expression. For the purpose of comparison, the data represented by the open bars were taken from Fig. 2E. Taken together, the data suggest that YFP- β 1 and CFP- γ 2 retain their ability to form a heterotrimer with $G\alpha_{oA}$.

Reconstitution of coupling between N-type Ca^{2+} channels and α 2-adrenergic receptors in neurons expressing PTX-resistant $G\alpha_{oA}$, YFP- β 1 and CFP- γ 2 subunits

The ability of tagged β 1 γ 2 to couple Ca^{2+} channels with α 2-ARs was also examined. In SCG neurons, α 2-ARs are coupled to N-type Ca^{2+} channels via PTX-sensitive G-proteins ($G\alpha_o$ or $G\alpha_i$; Schofield, 1990). In this set of

experiments, $G\alpha_{oA}$ (C351G) was co-expressed with tagged and untagged β 1 γ 2 in neurons pretreated overnight with PTX (500 ng ml⁻¹). The $G\alpha_{oA}$ (C351G) subunit contains a C-to-G mutation at the fourth amino acid from the C-terminus, which renders it PTX resistant (Milligan, 1988). In these reconstitution experiments, the results fell into three categories. First, greater expression levels of $G\alpha_{oA}$ (C351G) than either β 1 or γ 2 ($G\alpha_{oA} \gg G\beta$ 1 γ 2), resulted in $G\alpha_{oA}$ (C351G) serving as a 'buffer' (cf. Fig. 4B). This scenario is similar to the results presented in the previous section with GDP-bound $G\alpha_{oA}$. Second, greater expression levels of β 1 and γ 2 (β 1 γ 2 $\gg G\alpha_{oA}$) led to tonic Ca^{2+} channel inhibition and an increased basal facilitation

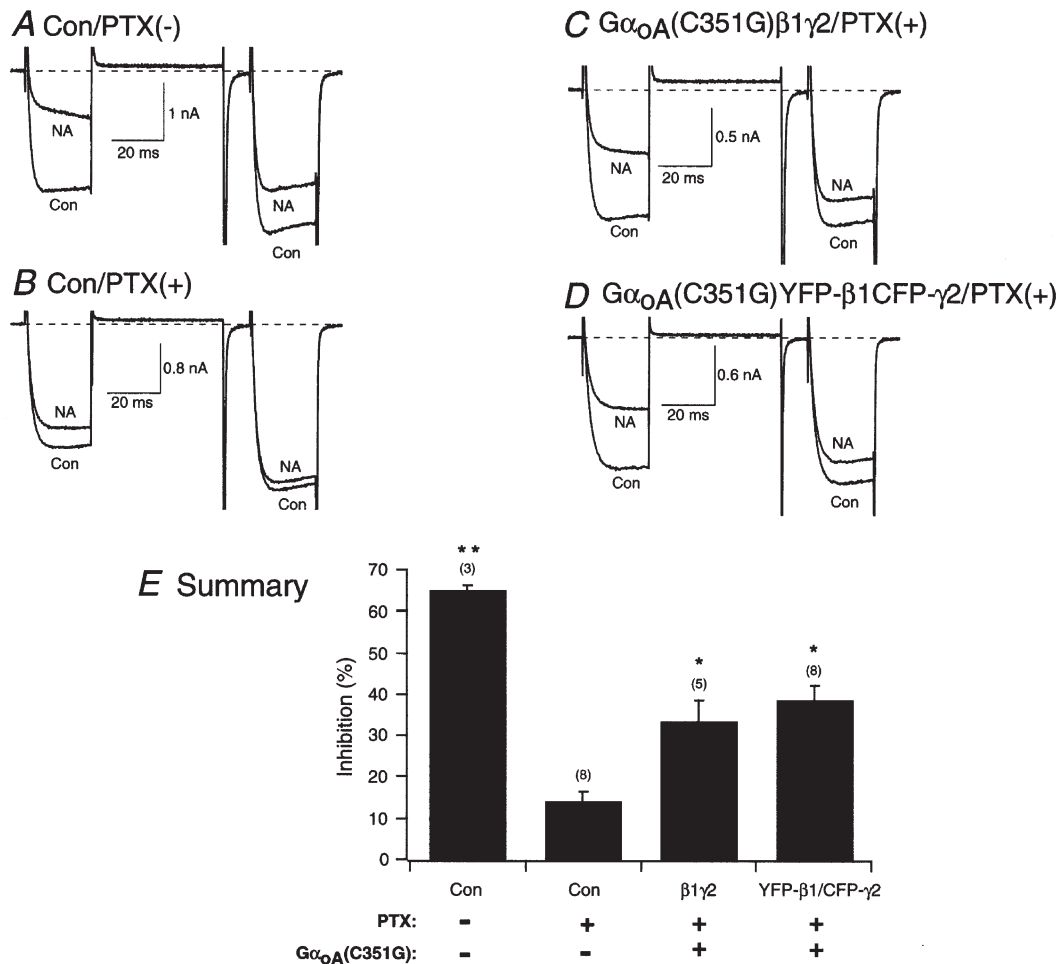


Figure 5. Reconstitution of α 2-adrenergic receptor coupling to N-type Ca^{2+} channels in SCG neurons expressing PTX-resistant $G\alpha_{oA}$ with β 1 γ or YFP- β 1/CFP- γ 2

Superimposed I_{Ca} traces evoked with the double-pulse voltage protocol (shown at the bottom of Fig. 2D) in the absence (lower traces) and presence (upper traces) of 10 μ M NA for control, no PTX (A), control plus PTX (500 ng ml⁻¹, overnight; B), PTX-pretreated neuron expressing $G\alpha_{oA}$ (C351G; C) and PTX-pretreated neuron co-expressing $G\alpha_{oA}$ (C351G) and YFP- β 1/CFP- γ 2 (D). Currents were evoked every 10 s. Dashed lines indicate the zero current level. E, summary graph of mean (\pm S.E.M.) NA-mediated I_{Ca} inhibition for uninjected (Con), $G\alpha_{oA}$ (C351G)/ β 1/ γ 2-expressing neurons and $G\alpha_{oA}$ (C351G)/YFP- β 1/CFP- γ 2-expressing neurons. NA-mediated inhibition was determined as described in the legend of Fig. 2. The final concentration of cDNA injected was 10 ng ml⁻¹ for the β and γ subunit, and 7 ng ml⁻¹ for the PTX-resistant α subunit. * P < 0.05 and ** P < 0.01 vs. PTX-treated control neurons. Numbers in parentheses indicate the number of experiments.

(cf. Fig. 2B–D; see also Ikeda, 1996; Ikeda & Dunlap, 1999). The third and essential outcome was a stoichiometric ‘balance’ of expression levels of all three microinjected subunits. Consequently, a criterion was employed whereby G-protein-expressing neurons with basal facilitation values ranging from 1.1 to 1.5 were included in the analysis (Jeong & Ikeda, 2000). As a result, 13 out of the 22 neurons co-injected with $G\alpha_{oA}$ (C351G) and untagged and tagged $\beta 1\gamma 2$ are described. In uninjected neurons, the application of NA inhibited I_{Ca} by $65.1 \pm 1.5\%$ ($n = 3$, $P < 0.01$ vs. PTX-treated control cells; Fig. 5A and E). Overnight pretreatment of uninjected neurons with PTX attenuated the NA-mediated I_{Ca} inhibition to $14.3 \pm 2.6\%$ ($n = 8$, Fig. 5B and E). Figure 5C shows superimposed I_{Ca} traces of a neuron co-injected with $G\alpha_{oA}$ (C351G) and $\beta 1\gamma 2$, exhibiting a basal facilitation of approximately 1.1. Upon exposure of the neuron to NA, I_{Ca} were inhibited by approximately 50%. In all five neurons tested, the mean I_{Ca} inhibition was $33.7 \pm 5.5\%$ ($P < 0.05$ vs. PTX-treated control cells; Fig. 5E). Superimposed I_{Ca} traces are illustrated in Fig. 5D from a neuron co-expressing $G\alpha_{oA}$ (C351G) and YFP- $\beta 1$ /CFP- $\gamma 2$, exhibiting a basal facilitation of 1.1. Following NA application, the current was inhibited by 47%. The mean current inhibition observed with $10 \mu\text{M}$ NA was $38.6 \pm 4.0\%$ ($n = 8$, $P < 0.05$ vs. PTX-treated control cells). Figure 5E summarizes the NA-mediated inhibition of I_{Ca} . When compared with uninjected neurons, the coupling efficiency was not as robust. One explanation may be that some of the neurons did not express sufficient amounts of ‘balanced’ G-protein subunits. However, the lack of an assay to quantify expression levels makes it difficult to interpret these differences. Nonetheless, these results lend support to the notion that coupling between $\alpha 2$ -ARs and N-type Ca^{2+} channels is partially reconstituted in neurons expressing tagged $\beta 1\gamma 2$ and PTX-resistant $G\alpha_{oA}$. Similar observations with several untagged $\beta\gamma$ combinations have been reported previously by Jeong & Ikeda (2000) under conditions where a ‘balance’ between $G\alpha$ and $G\beta\gamma$ subunit expression was obtained.

FRET analysis of co-expressed YFP- $\beta 1$ and CFP- $\gamma 2$ in SCG neurons

FRET was employed to examine the *in vivo* interaction between YFP- $\beta 1$ and CFP- $\gamma 2$. In this set of experiments, YFP- $\beta 1$ and CFP- $\gamma 2$ were injected at a concentration of $10 \text{ ng } \mu\text{l}^{-1}$ per subunit. FRET involves the transfer of energy from an excited fluorophore (donor) to a second fluorophore (acceptor) in a non-radiative manner. Thus, when the donor is excited at the proper wavelength, the acceptor produces an emission, there being a concomitant decrease in donor emission. Although YFP and CFP are the most commonly used GFP pairs, the two fluorophores possess some overlapping spectra that are susceptible to cross-talk (bleed-over). The amount of cross-talk due to the two fluorophores cannot be measured directly in cells expressing YFP and CFP. It can, however, be determined in cells expressing either YFP or CFP alone. In CFP-

expressing neurons, excitation (at 440 nm) of the fluorophore with the FRET filter results in CFP emission (at 480 nm) through the donor filter (Dd). Donor cross-talk (or Fd) is the CFP emission (at 535 nm) leaking through the acceptor filter. Figure 6A shows the Fd CFP emission as a function of the Dd CFP emission in neurons expressing ECFP (filled circles) or $\beta 1$ /CFP- $\gamma 2$ (open circles). Both sets of emission data were fitted to a straight line. The slopes (Fd/Dd) of the lines for ECFP- and $\beta 1$ /CFP- $\gamma 2$ -expressing cells were 0.300 ± 0.002 ($n = 9$, dashed line) and 0.292 ± 0.004 ($n = 11$, continuous line), respectively. Figure 6A also illustrates that given the broad range of expression values for either ECFP or CFP- $\gamma 2$, the contribution of donor cross-talk remains relatively constant ($\sim 30\%$).

Acceptor (YFP) cross-talk occurs when YFP-expressing cells are excited (at 440 nm) with the FRET filter and emission occurs at 535 nm (Fa). That is, there is a direct excitation of the acceptor by the FRET filter. Figure 6B shows a plot of Fa YFP emission as a function of Aa YFP emission measured at 535 nm when the cells were excited at 500 nm with the acceptor filter. The Fa/Aa ratios of EYFP- (filled circles) and YFP- $\beta 1\gamma 2$ -expressing cells (open circles) were 0.229 ± 0.013 ($n = 6$, dashed line) and 0.219 ± 0.005 ($n = 9$, continuous line), respectively. This reflects YFP cross-talk of approximately 22%. Note that the scaling for the YFP (acceptor) plot (Fig. 6B) is different from that of the CFP (donor) graph (Fig. 6A). One possible explanation for this discrepancy may be that different filters were used to record emission signals for each fluorophore. Nonetheless, as observed with CFP-expressing neurons, the contribution of YFP cross-talk remains constant with varying fluorophore expression levels (Fig. 6B).

Figure 6C shows a plot of the emission signal measured at 535 nm (Ff) as a function of the signal measured at 480 nm (Df), employing the FRET filter, in neurons co-expressing the non-interacting fluorophores ECFP and EYFP (open triangles). Both Ff and Df emission values have been corrected for cross-talk in all groups. Thus, the Ff/Df ratio is a measure of FRET. The Ff and Df emission values for cells co-expressing EYFP/ECFP, and YFP- $\beta 1$ /CFP- $\gamma 2$ with 50 or $100 \text{ ng } \mu\text{l}^{-1}$ $\beta 1$ were pooled and fitted with a straight-line equation. The slope of the fitted line was 0.316 ± 0.011 ($n = 18$, continuous line). The emission of neurons co-expressing YFP- $\beta 1$ /CFP- $\gamma 2$ (filled circles) is also shown in Fig. 6C. Fitting these points to a straight line resulted in a slope value of 0.364 ± 0.029 ($n = 15$, dashed line). To determine whether the change in slope could be attributed to FRET, it was necessary to disrupt the number of YFP- $\beta 1$ /CFP- $\gamma 2$ complexes expressed. $G\beta\gamma$ is a tightly bound functional monomer that dissociates when exposed to strong denaturants (Schmidt & Neer, 1991). Thus, this permanent interaction precluded our ability to disrupt the monomer and measure pre-FRET values within the same cells. An alternative approach was to co-inject untagged $\beta 1$ at

higher concentrations than YFP- $\beta 1$ and CFP- $\gamma 2$, to increase the expression of $\beta 1$ /CFP- $\gamma 2$ dimers. The Ff and Df emission values for cells expressing 5-fold (open squares) and 10-fold (open circles) higher untagged $\beta 1$ with YFP- $\beta 1$ /CFP- $\gamma 2$ were not different from the values of EYFP/ECFP-expressing cells. As mentioned above, the emission data for all three groups were pooled and the majority of these values fell remarkably along the fitted line. This result suggests that similar to cells expressing the non-interacting fluorophores (ECFP/EYFP), co-injection of higher concentrations of untagged $\beta 1$ cDNA leads to a decrease in dimer formation between both YFP- $\beta 1$ and CFP- $\gamma 2$. Figure 6D is a bar plot of the mean FRET values of the four groups of cells. Neurons co-expressing YFP- $\beta 1$ /CFP- $\gamma 2$ had a significantly greater FRET value than cells co-expressing the non-interacting fluorophores (0.317 ± 0.007 , $n = 5$ vs. 0.452 ± 0.013 , $n = 15$, $P < 0.01$).

Furthermore, co-injecting 50 or 100 $\text{ng } \mu\text{l}^{-1}$ of untagged $\beta 1$ cDNA significantly ($P < 0.01$) decreased the FRET value to 0.324 ± 0.008 ($n = 5$) and 0.291 ± 0.005 ($n = 8$), respectively (Fig. 6D). Taken together, these results provide evidence that co-expressed YFP- $\beta 1$ and CFP- $\gamma 2$ interact *in vivo* and are 10–100 Å (1–10 nm) apart; this is the distance required for FRET to occur.

DISCUSSION

GPCRs modulate voltage-gated Ca^{2+} channels via several different pathways. The most common and best-studied pathway involves P/Q- or N-type Ca^{2+} channel inhibition that is both voltage dependent and membrane delimited. Components in this pathway involve a GPCR, heterotrimeric G-protein (i.e. $G\alpha\beta\gamma$) and Ca^{2+} channels (effector). Following receptor activation, the heterotrimer

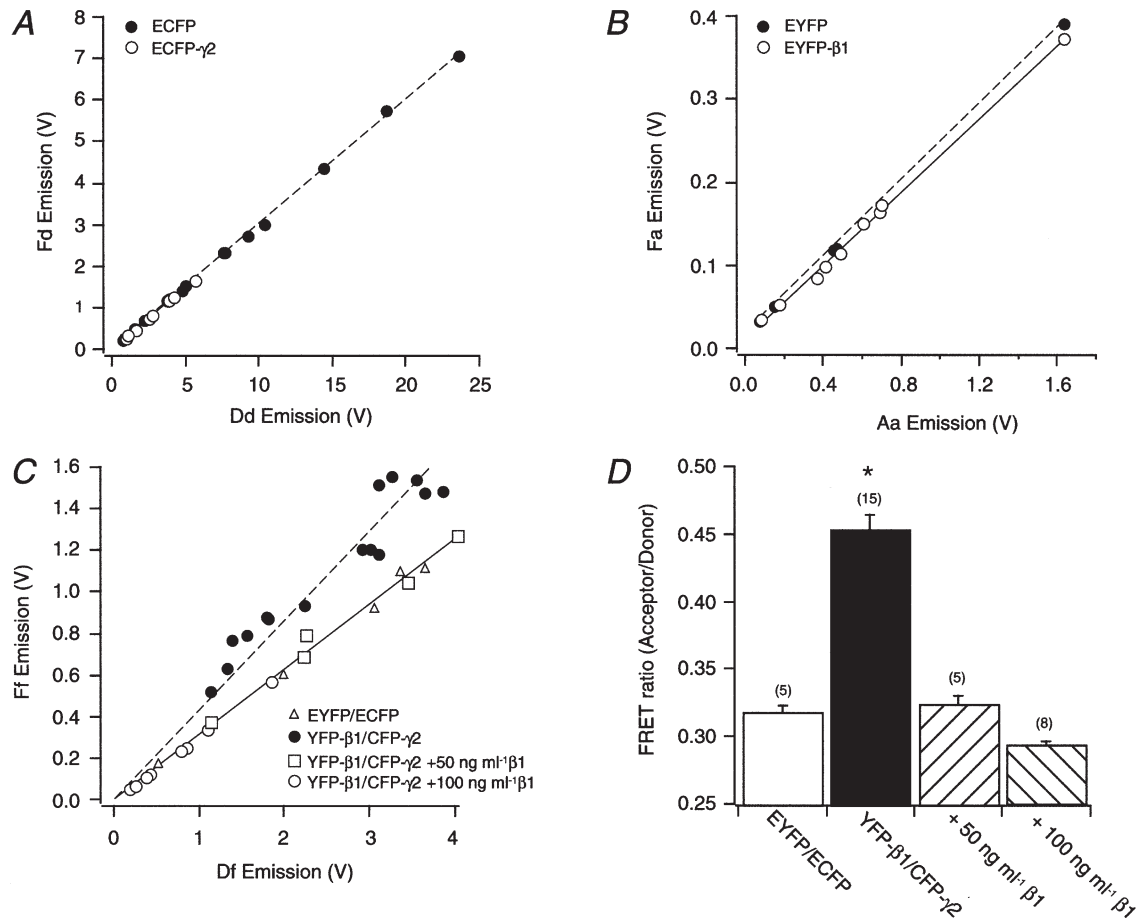


Figure 6. Calculation of FRET values in SCG neurons expressing ECFP, CFP- $\gamma 2$, EYFP and YFP- $\beta 1$

Emissions recorded in SCG neurons expressing ECFP (filled circles) and E $\beta 1$ /CFP- $\gamma 2$ (open circles; A), EYFP (filled circles) and EYFP- $\beta 1$ / $\gamma 2$ (open circles; B) and EYFP/ECFP (open triangles), YFP- $\beta 1$ /CFP- $\gamma 2$ (filled circles), YFP- $\beta 1$ /CFP- $\gamma 2$ + 50 ng ml^{-1} $\beta 1$ (open squares) and YFP- $\beta 1$ /CFP- $\gamma 2$ + 100 ng ml^{-1} $\beta 1$ (open circles; C). Emission values were determined as described in Methods. Dashed and continuous lines represent best fits to a straight-line equation. D, summary graph of mean (\pm S.E.M.) FRET values for neurons expressing EYFP/ECFP, YFP- $\beta 1$ /CFP- $\gamma 2$, YFP- $\beta 1$ /CFP- $\gamma 2$ + 50 ng ml^{-1} $\beta 1$ and YFP- $\beta 1$ /CFP- $\gamma 2$ + 100 ng ml^{-1} $\beta 1$. * $P < 0.01$ vs. EYFP/ECFP-expressing cells. Numbers in parentheses indicate the number of experiments.

dissociates into free $G\alpha$ and $G\beta\gamma$ subunits, both of which can modulate several effectors. $G\beta\gamma$ subunits mediate the voltage-dependent modulation (Herlitze *et al.* 1996; Ikeda, 1996). Biochemical assays have expanded on these observations by demonstrating an interaction of the Ca^{2+} channel α_1 subunit with $G\beta\gamma$ (De Waard *et al.* 1997; Zamponi *et al.* 1997; Qin *et al.* 1997; Furukawa *et al.* 1998; Canti *et al.* 1999). At present, evidence for a direct *in vivo* interaction of $G\beta\gamma$ and Ca^{2+} channels is lacking.

GFP from the jellyfish *Aequoria* has become a widely employed tag for the study of protein synthesis and trafficking in living cells (Feng *et al.* 1998; Li *et al.* 1999). GFP has also served as an important tool in monitoring protein–protein interactions using FRET technology (Mahajan *et al.* 1998; Vanderklish *et al.* 2000). The crystal structure of GFP shows that it is a cylindrical structure made up of eleven strands of β -sheets with an α -helix running up the axis of the cylinder (Ormo *et al.* 1996; Yang *et al.* 1996). It is within this cylinder that the chromophore is buried. We wanted to take advantage of the unique spectral abilities of the two GFP mutants (YFP and CFP) to study G-protein subunit cell signalling mechanisms with regard to N-type Ca^{2+} channel modulation. YFP and CFP were fused in-frame to $G\beta 1$ and $G\gamma 2$, respectively. Therefore, the purpose of the present study was to determine whether intranuclear microinjection of YFP- $\beta 1$ and CFP- $\gamma 2$ cDNA constructs would result in the functional expression of both subunits. In particular, we wanted to ascertain whether YFP- $\beta 1$ /CFP- $\gamma 2$ would interact with effectors, form a heterotrimer and couple to native $\alpha 2$ -ARs. Furthermore, FRET technology was employed to ascertain whether the two fluorophores were in close proximity and in the appropriate orientation to allow them to interact.

The crystal structures of $G\alpha\beta\gamma$ and free $G\beta\gamma$ have recently been elucidated (Wall *et al.* 1995; Lambright *et al.* 1996). These reports have shown that the β subunit is composed of an N-terminal α helix that is followed by a torus (seven-bladed propeller-like structure) composed of the ‘top’ and ‘bottom’ surfaces, outer surface and the surface that lines the tunnel of the protein. $G\alpha$ contacts $G\beta$ at the ‘top’ surface of the torus and the first blade of the propeller. The $G\gamma$ subunit is prenylated at the C-terminus and is tightly bound to blades 1, 5, 6 and 7 of $G\beta$. Ford *et al.* (1998) performed mutational analysis of sites on $G\beta 1$ that interact with several effectors including N-type Ca^{2+} and GIRK channels. The introduction of point mutations on the torus revealed regions on $G\beta$ that were important for effector interaction and heterotrimer formation. However, the effect of point mutations on residues along the N-terminus was not examined. Based on the crystal structure of the $G\alpha\beta\gamma$ heterotrimer, it was possible to speculate on the spatial orientation of both fluorophores fused to the N-termini of $\beta 1$ and $\gamma 2$. However, whether CFP and YFP would be in close proximity and in the proper orientation for FRET to occur was uncertain. Furthermore, due to the ability of

$G\beta\gamma$ to modulate several effectors, it was also unclear how tagging both subunits with a 238 amino acid protein (~ 28 kDa) would alter their function.

Intranuclear microinjection of YFP- $\beta 1$ and CFP- $\gamma 2$ cDNA constructs into SCG neurons resulted in the expression of both subunits when co-injected together or with the untagged form of the other subunit (Fig. 1). The distribution of these subunits appeared to be membrane bound. However, the presence of cytoplasmic tagged subunits cannot be ruled out. For instance, Jin *et al.* (2000) tagged the $G\beta$ subunit of *Dictyostelium discoideum* with GFP and found approximately 70% of $G\beta$ to be membrane bound. In the present study, for the most part, the fluorescence was homogeneous, without a punctate appearance, and was not distributed within specific organelles.

The functional properties of the YFP- $\beta 1$ and CFP- $\gamma 2$ subunits were tested and compared with those of untagged $\beta 1\gamma 2$. $G\beta\gamma$ subunits are now well established as entities that act on several effectors, including N- and P/Q-type Ca^{2+} channels, GIRK channels, phospholipase $C\beta$ and several receptor kinases (Clapham & Neer, 1997). The results presented in Fig. 2 demonstrate the ability of the tagged subunits to interact with Ca^{2+} channels in a similar manner to untagged $\beta 1$ and $\gamma 2$. That is, when these two subunits were co-injected, there was a significant increase in basal facilitation when compared to uninjected neurons. Expression of YFP- $\beta 1$ alone resulted in a significant increase in basal facilitation, but its magnitude was not greater than when the two subunits were co-expressed together. Similar to our previous study (Ruiz-Velasco & Ikeda, 2000), heterologous expression of the $\gamma 2$ subunit alone did not lead to a significant change in Ca^{2+} channel basal facilitation. In fact, the β and γ subunits, either tagged or untagged, must be co-expressed in order to observe the optimal modulation of N-type Ca^{2+} channels.

GIRK channels are also regulated by direct interaction with $G\beta\gamma$ subunits (Logothetis *et al.* 1987; Jan & Jan, 1997). With the exception of $G\beta 5$, there now appears to be little $\beta\gamma$ specificity with regard to GIRK channel activation (Lei *et al.* 2000). Previously, we had shown that heterologous overexpression of $\beta 1\gamma 2$ and GIRK channels in SCG neurons resulted in tonic channel activation (Ruiz-Velasco & Ikeda, 2000). In the present study we extended our observations by showing that the tagged subunits were also capable of tonically activating GIRK channels (Fig. 3). Significant basal activation was observed only after co-expressing either tagged or untagged β and γ subunits. Similar observations have been made in HEK cells stably expressing GIRK1 and GIRK4 channels (Lei *et al.* 2000). Cotransfection of HEK cells with $\beta 1$, $\beta 3$ or $\beta 4$ with $\gamma 2$ resulted in enhanced GIRK channel currents when compared to untransfected cells. Both GFP-tagged subunits, therefore, showed the ability to modulate both effectors (e.g. N-type Ca^{2+} and GIRK channels).

Whether YFP- $\beta 1$ and CFP- $\gamma 2$ were capable of interacting with $G\alpha$ subunits was also tested in this study. The approach employed was the overexpression of $G\alpha_{oA}$ at higher amounts than either the tagged or untagged $\beta 1$ or $\gamma 2$ subunits. Because the excess GDP-bound $G\alpha_{oA}$ has a higher affinity for $\beta\gamma$ subunits, any $\beta\gamma$ -mediated effects are suppressed (Slepak *et al.* 1995; Ikeda, 1996). The summary in Fig. 4E shows that overexpression of $G\alpha_{oA}$ in SCG neurons alone or with untagged $\beta 1\gamma 2$ significantly decreased the NA-mediated calcium current inhibition. Similar results regarding N-type Ca^{2+} channel modulation with several $G\alpha$ subunits, including $G\alpha_{oA}$, have previously been reported by Jeong & Ikeda (1999). Moreover, the suppression by excess $G\alpha_{oA}$ of several other effectors has been shown for GIRK channels (Ito *et al.* 1992; Reuveny *et al.* 1994) and phospholipase $C\beta$ (Katz *et al.* 1992).

Having demonstrated the ability of YFP- $\beta 1$ and CFP- $\gamma 2$ to form a heterotrimer with $G\alpha_{oA}$, we examined whether the heterotrimer would couple to native $\alpha 2$ -ARs and modulate N-type I_{Ca} . Under conditions where all three subunits were expressed in a 1:1:1 ratio (see Results), the reconstitution of NA-mediated I_{Ca} inhibition was observed (Fig. 5). The reconstitution observed with both tagged and untagged subunits was not as robust as for control neurons. Such differences in coupling efficiency may have been due to the C351G mutation on $G\alpha_{oA}$ affecting the manner in which it couples to $\alpha 2$ -ARs. Alternatively, there may have been some competition for 'access' to receptors between native and heterologously expressed G-protein subunits. Another explanation may involve differences in G-protein expression levels. We are as yet unable to quantify expressed protein levels. Nonetheless, these results are in agreement with those presented by Jeong & Ikeda (2000) and indicate that tagged $\beta 1$ and $\gamma 2$ subunits are capable of coupling to $\alpha 2$ -ARs.

Tagging proteins with GFP has now become an extremely useful method for measuring the dynamic interactions between proteins. Employing FRET technology accomplishes this task. In order for FRET to occur, the two fluorophores need to be in close proximity (10–100 Å) and in the proper orientation. One of the most successful FRET pairs is CFP (donor) and YFP (acceptor). However, a limitation of this pair is the overlying spectra, which causes a poor separation between donor and acceptor emissions (Pollok & Heim, 1999). The Fd and Ad signals (see Methods for description) represent CFP cross-talk, while the Fa and Da signals represent cross-talk due to YFP. Employing the proper filter sets minimizes this problem. In the present study, for instance, the values for both Ad and Da were effectively zero. Moreover, the contribution of CFP (Fd) and YFP (Fa) cross-talk was approximately 30 and 22%, respectively (Fig. 6A and B). FRET measurements (Ff/Df, Fig. 6C) provided evidence that suggests there is a stable interaction between co-expressed YFP- $\beta 1$ and CFP- $\gamma 2$. Given the molecular

interaction between the two subunits, it was not possible to measure FRET under conditions where the two subunits are naturally apart (Schmidt & Neer, 1991). Nonetheless, the disruption of the two tagged subunits was achieved indirectly by co-injecting a 5-fold and 10-fold higher amount of untagged $G\beta 1$ cDNA (Fig. 6). This resulted in a significant decrease in FRET values, which were not different from those of cells expressing non-interacting fluorophores (EYFP and ECFP). In fact, Fig. 6C shows that all emission values of neurons co-expressing YFP- $\beta 1$ /CFP- $\gamma 2$ (filled circles) within the given emission range were greater than those of the other three groups of cells. Furthermore, a shift in the slope of the fitted line was observed. Since all values plotted have been corrected for cross-talk, the most plausible explanation for this change is the occurrence of FRET between the two fluorophores.

In a recent study, the functional interaction between $G\beta$ -YFP and $G\alpha 2$ -CFP in *Dictyostelium discoideum* was undertaken successfully (Janetopoulos *et al.* 2001). The authors reported the occurrence of FRET between the two G-protein subunits. In this study, we found that tagging $\beta 1$ and $\gamma 2$ with YFP and CFP, respectively, did not interfere with their ability to modulate N-type Ca^{2+} channels. Since this modulation is believed to be the result of a direct interaction between $G\beta\gamma$ and Ca^{2+} channels, the next step would be to determine whether FRET occurs between one of the tagged G-proteins and tagged Ca^{2+} channels. Indeed, Witteman *et al.* (2000) have reported recently the successful expression of Ca^{2+} channel $\beta 4$ subunits tagged with GFP to the N-terminus. Alternatively, the ability to measure levels of expressed GFP-tagged proteins can be accomplished with the aid of spectroscopy or confocal microscopy.

In summary, our results show the successful heterologous expression of YFP- $G\beta 1$ and CFP- $\gamma 2$ subunits in rat SCG neurons. Similar to untagged $\beta 1\gamma 2$ subunits, YFP- $\beta 1$ /CFP- $\gamma 2$ co-expression resulted in basal N-type I_{Ca} inhibition and GIRK channel activation. In addition, heterotrimer formation was observed under conditions whereby excess GDP-bound $G\alpha_{oA}$ was co-expressed with both tagged subunits. Evidence for $\alpha 2$ -AR coupling to $G\alpha_{oA}$ (C351G)/YFP- $\beta 1$ /CFP- $\gamma 2$ was provided. And finally, this study utilized FRET technology for monitoring protein–protein interactions between G-protein subunits.

- ARNOT, M. I., STOTZ, S. C., JARVIS, S. E. & ZAMPONI, G. W. (2000). Differential modulation of N-type 1B and P/Q-type 1A calcium channels by different G protein subunit isoforms. *Journal of Physiology* **527**, 203–212.
- CANTI, C., PAGE, K. M., STEPHENS, G. J. & DOLPHIN, A. C. (1999). Identification of residues in the N-terminus of $\alpha 1B$ critical for inhibition of the voltage-dependent potassium channel by $G\beta\gamma$. *Journal of Neuroscience* **19**, 6855–6864.

- CAULFIELD, M. P., JONES, S., VALLIS, Y., BUCKLEY, N. J., KIM, G., MILLIGAN, G. & BROWN, D. A. (1994). Muscarinic M-current inhibition via G $\alpha_{q/11}$ and α -adrenoceptor inhibition of Ca²⁺ current via G α , in rat sympathetic neurones. *Journal of Physiology* **477**, 415–422.
- CLAPHAM, D. E. & NEER, E. J. (1997). G protein $\beta\gamma$ subunits. *Annual Review of Pharmacology and Toxicology* **37**, 167–203.
- DE WAARD, M., LIU, H., WALKER, D., SCOTT, V. E., GURNETT, C. A. & CAMPBELL, K. P. (1997). Direct binding of G-protein $\beta\gamma$ complex to voltage-dependent calcium channels. *Nature* **385**, 446–450.
- DOLPHIN, A. C. (1998). Mechanisms of modulation of voltage-dependent calcium channels by G proteins. *Journal of Physiology* **50**, 3–11.
- FENG, X., ZHANG, J., BARAK, L. S., MEYER, T., CARON, M. G. & HANNUN, Y. A. (1998). Visualization of dynamic trafficking of a protein kinase C β II/green fluorescent protein conjugate reveals differences in G protein-coupled receptor activation and desensitization. *Journal of Biological Chemistry* **273**, 10755–10762.
- FERNANDEZ-FERNANDEZ, J. M., WANAVERBEQ, N., HALLEY, P., CAULFIELD, M. P. & BROWN, D. A. (1999). Selective activation of heterologously expressed G protein-gated K⁺ channels by M2 muscarinic receptors in rat sympathetic neurones. *Journal of Physiology* **515**, 631–637.
- FORD, C. E., SKIBA, N. P., BAE, H., DAAKA, Y., REUVENY, E., SHEKTER, L. R., ROSAL, R., WENG, G., YANG, C. S., IYENGAR, R., MILLER, R. J., JAN, L. Y., LEFKOWITZ, R. J. & HAMM, H. E. (1998). Molecular basis for interactions of G protein $\beta\gamma$ subunits with effectors. *Science* **280**, 1271–1274.
- FURUKAWA, T., MIURA, R., MORI, Y., STROBECK, M., SUZUKI, K., OGIHARA, Y., ASANO, T., MORISHITA, R., HASHII, M., HIGASHIDA, H., YOSHII, M. & NUKADA, T. (1998). Differential interactions of the C terminus and the cytoplasmic I-II loop of neuronal Ca²⁺ channels with G-protein α and $\beta\gamma$ subunits. II. Evidence for direct binding. *Journal of Biological Chemistry* **273**, 17595–17603.
- GORDON, G. W., BERRY, G., LIANG, H. L., LEVINE, B. & HERMAN, B. (1998). Quantitative fluorescence resonance energy transfer measurements using fluorescence microscopy. *Biophysical Journal* **74**, 2702–2713.
- HAMILL, O. P., MARTY, A., NEHER, E., SAKMANN, B. & SIGWORTH, F. J. (1981). Improved patch-clamp techniques for high-resolution recording from cells and cell-free membrane patches. *Pflügers Archiv* **391**, 85–100.
- HERLITZE, S., GARCIA, D. E., MACKIE, K., HILLE, B., SCHEUER, T. & CATTERALL, W. A. (1996). Modulation of Ca²⁺ channels by G-protein $\beta\gamma$ subunits. *Nature* **380**, 258–262.
- HILLE, B. (1994). Modulation of ion-channel function by G-protein-coupled receptors. *Trends in Neurosciences* **17**, 531–536.
- HUANG, C. L., SLESINGER, P. A., CASEY, P. J., JAN, Y. N. & JAN, L. Y. (1995). Evidence that direct binding of G $\beta\gamma$ to the GIRK1 G protein-gated inwardly rectifying K⁺ channel is important for channel activation. *Neuron* **15**, 1133–1143.
- IKEDA, S. R. (1991). Double-pulse calcium channel current facilitation in adult rat sympathetic neurones. *Journal of Physiology* **439**, 181–214.
- IKEDA, S. R. (1996). Voltage-dependent modulation of N-type calcium channels by G-protein $\beta\gamma$ subunits. *Nature* **380**, 255–258.
- IKEDA, S. R. (1997). Heterologous expression of receptors and signaling proteins in adult mammalian sympathetic neurons by microinjection. In *Methods in Molecular Biology: Receptor Signal Transduction Protocols*, vol. 83, ed. CHALLIS, R. A. J., pp. 191–202. Human, Totowa, NJ, USA.
- IKEDA, S. R. & DUNLAP, K. (1999). Voltage-dependent modulation of N-type calcium channels: Role of G protein subunits. *Advances in Second Messenger and Phosphoprotein Research* **33**, 131–151.
- ITO, H., TUNG, R. T., SUGIMOTO, T., KOBAYASHI, I., TAKAHASHI, K., KATADA, T., UI, M. & KURACHI, Y. (1992). On the mechanism of G protein $\beta\gamma$ subunit activation of the muscarinic K⁺ channel in guinea pig atrial cell membrane. *Journal of General Physiology* **99**, 961–983.
- JAN, L. Y. & JAN, Y. N. (1997). Voltage-gated and inwardly rectifying potassium channels. *Journal of Physiology* **505**, 267–282.
- JANETPOULOS, C., JIN, T. & DEVREOTES, P. (2001). Receptor-mediated activation of heterotrimeric G-proteins in living cells. *Science* **291**, 2408–2411.
- JEONG, S. W. & IKEDA, S. R. (1999). Sequestration of G-protein $\beta\gamma$ subunits by different G-protein α subunits blocks voltage-dependent modulation of Ca²⁺ channels in rat sympathetic neurons. *Journal of Neuroscience* **19**, 4755–4761.
- JEONG, S. W. & IKEDA, S. R. (2000). Effect of G protein heterotrimer composition on coupling of neurotransmitter receptors to N-type Ca²⁺ channel modulation in sympathetic neurons. *Proceedings of the National Academy of Sciences of the USA* **97**, 907–912.
- JIN, T., ZHANG, N., LONG, L., PARENT, C. A. & DEVREOTES, P. N. (2000). Localization of the G protein $\beta\gamma$ complex in living cells during chemotaxis. *Science* **287**, 1034–1036.
- KATZ, A., WU, D. & SIMON, M. I. (1992). Subunits $\beta\gamma$ of heterotrimeric G proteins activate β 2 isoform of phospholipase C. *Nature* **360**, 686–689.
- KOFUJI, P., DAVIDSON, N. & LESTER, H. A. (1995). Evidence that neuronal G-protein-gated inwardly rectifying K⁺ channels are activated by G $\beta\gamma$ subunits and function as heteromultimers. *Proceedings of the National Academy of Sciences of the USA* **92**, 6542–6546.
- LAMBRIGHT, D. G., SONDEK, J., BOHM, A., SKIBA, N. P., HAMM, H. E. & SIGLER, P. B. (1996). The 2.0 Å crystal structure of a heterotrimeric G protein. *Nature* **379**, 311–319.
- LEI, Q., JONES, M. B., TALLEY, E. M., SCHRIER, A. D., MCINTIRE, W. E., GARRISON, J. C. & BAYLISS, D. A. (2000). Activation and inhibition of G protein-coupled inwardly rectifying potassium (Kir3) channels by G protein $\beta\gamma$ subunits. *Proceedings of the National Academy of Sciences of the USA* **97**, 9771–9776.
- LI, C. J., HEIM, R., LU, P., TSIEN, R. Y. & CHANG, D. C. (1999). Dynamic redistribution of calmodulin in HeLa cells during cell division as revealed by a GFP-calmodulin fusion protein technique. *Journal of Cell Science* **112**, 1567–1577.
- LOGOTHETIS, D. E., KURACHI, Y., GALPER, J., NEER, E. J. & CLAPHAM, D. E. (1987). The $\beta\gamma$ subunits of GTP-binding proteins activate the muscarinic K⁺ channel in heart. *Nature* **325**, 321–326.
- MAHAJAN, N. P., LINDER, K., BERRY, G., GORDON, G. W., HEIM, R. & HERMAN, B. (1998). Bcl-2 and Bax interactions in mitochondria probed with green fluorescent protein and fluorescence resonance energy transfer. *Nature Biotechnology* **16**, 547–551.
- MILLIGAN, G. (1988). Techniques used in the identification and analysis of function of pertussis toxin-sensitive guanine nucleotide binding proteins. *Biochemical Journal* **255**, 1–13.
- ORMO, M., CUBITT, A. B., KALLIO, K., GROSS, L. A., TSIEN, R. Y. & REMINGTON, S. J. (1996). Crystal structure of the *Aequorea victoria* green fluorescent protein. *Science* **273**, 1392–1395.
- POLLOK, B. A. & HEIM, R. (1999). Using GFP in FRET-based applications. *Trends in Cell Biology* **9**, 57–60.

- QIN, N., PLATANO, D., OLCESE, R., STEFANI, E. & BIRNBAUMER, L. (1997). Direct interaction of G $\beta\gamma$ with a C-terminal G $\beta\gamma$ -binding domain of the Ca²⁺ channel α_1 subunit is responsible for channel inhibition by G protein-coupled receptors. *Proceedings of the National Academy of Sciences of the USA* **94**, 8866–8871.
- REUVENY, E., SLESINGER, P. A., INGLESE, J., MORALES, J. M., INIGUEZ-LLUHI, J. A., LEFKOWITZ, R. J., BOURNE, H. R., JAN, Y. N. & JAN, L. Y. (1994). Activation of the cloned muscarinic potassium channel by G protein $\beta\gamma$ subunits. *Nature* **370**, 143–146.
- RUIZ-VELASCO, V. & IKEDA, S. R. (1998). Heterologous expression and coupling of G protein-gated inwardly rectifying K⁺ channels in rat sympathetic neurons. *Journal of Physiology* **513**, 761–773.
- RUIZ-VELASCO, V. & IKEDA, S. R. (2000). Multiple G-protein $\beta\gamma$ combinations produce voltage-dependent inhibition of N-type calcium channels in rat superior cervical ganglion neurons. *Journal of Neuroscience* **20**, 2183–2191.
- SCHMIDT, C. J. & NEER, E. J. (1991). *In vitro* synthesis of G protein $\beta\gamma$ dimers. *Journal of Biological Chemistry* **266**, 4538–4544.
- SCHOFIELD, G. G. (1990). Norepinephrine blocks a calcium current of adult rat sympathetic neurons via an α_2 -adrenoceptor. *European Journal of Pharmacology* **180**, 37–47.
- SLEPAK, V. Z., KATZ, A. & SIMON, M. I. (1995). Functional analysis of a dominant negative mutant of G α_{i2} . *Journal of Biological Chemistry* **270**, 4037–4041.
- TSIEN, R. (1998). The green fluorescent protein. *Annual Review of Biochemistry* **67**, 509–544.
- VANDERKLISH, P. W., KRUSHEL, L. A., HOLST, B. H., GALLY, J. A., CROSSIN, K. L. & EDELMAN, G. M. (2000). Marking synaptic activity in dendritic spines with a calpain substrate exhibiting fluorescence resonance energy transfer. *Proceedings of the National Academy of Sciences of the USA* **97**, 2253–2258.
- WALL, M. A., COLEMAN, D. E., LEE, E., INIGUEZ-LLUHI, J. A., POSNER, B. A., GILMAN, A. G. & SPRANG, S. R. (1995). The structure of the G protein heterotrimer Gi $\alpha_1\beta_1\gamma_2$. *Cell* **83**, 1047–1058.
- WITTEMANN, S., MARK, M. D., RETTIG, J. & HERLITZE, S. (2000). Synaptic localization and presynaptic function of calcium channel β_4 -subunits in cultured hippocampal neurons. *Journal of Biological Chemistry* **275**, 37807–37814.
- YANG, F., MOSS, L. G. & PHILLIPS, G. M. (1996). The molecular structure of green fluorescent protein. *Nature Biotechnology* **14**, 1246–1252.
- ZAMPONI, G. W., BOURINET, E., NELSON, D., NARGEOT, J. & SNUTCH, T. P. (1997). Crosstalk between G proteins and protein kinase C mediated by the calcium channel α_1 subunit. *Nature* **385**, 442–446.
- ZHOU, J. Y., SIDEROVSKI, D. P. & MILLER, R. J. (2000). Selective regulation of N-type Ca channels by different combinations of G-protein β/γ subunits and RGS proteins. *Journal of Neuroscience* **20**, 7143–7148.

Acknowledgements

We thank Marina M. King and Linda Olmstead for their excellent technical assistance, and the following for providing cDNA clones: Dr R. J. Miller for YFP-G β_1 , Dr M. I. Simon for β_1 and γ_2 and Dr D. E. Logothetis for GIRK1 and GIRK4. This work was supported by grants from the National Institutes of Health (grant nos GM 56180 to S.R.I. and MH12288 to V.R.-V.).

Corresponding author

V. Ruiz-Velasco: Laboratory of Molecular Physiology, Guthrie Research Institute, 1 Guthrie Square, Sayre, PA 18840, USA.

Email: vruizvel@inet.guthrie.org